

# Constrained Model Predictive Control Based on Event Triggering for the Rare Earth Extraction Process

Zhiyong Zhang, Jianyong Zhu,\* Cong Xiong, Hui Yang, and Feiping Nie



Cite This: *ACS Omega* 2023, 8, 41943–41952

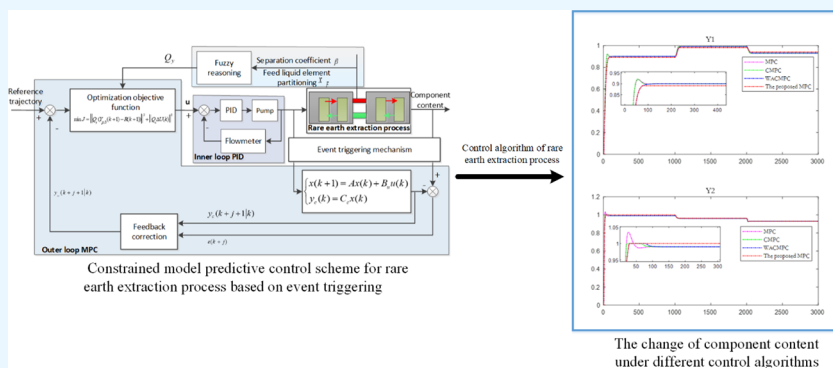


Read Online

ACCESS |

Metrics & More

Article Recommendations



**ABSTRACT:** Since the reagent dosage is manually adjusted according to work conditions, an event-triggered constrained model predictive control is proposed for rare earth extraction. First, the linear predictive system, based on a state space model, is established. Subsequently, the feedback correction link is fine-tuned to reduce the prediction error. Following this, an objective optimization function, incorporating input and output constraints, is introduced to calculate the appropriate reagent dosage. Finally, an event-triggering mechanism, underpinned by a designated threshold, is designed to update the controller. Simulation outcomes substantiate the efficacy of the proposed approach.

## INTRODUCTION

Rare earth elements, colloquially referred to as “industrial vitamins”, have escalated into crucial strategic resources. Although China’s theoretical grasp of the rare earth extraction process has reached global prominence,<sup>1</sup> the automation level within the industry remains subpar. This shortfall results in diminished production efficiency, extensive resource consumption, and inconsistent product quality, thereby hindering expansion of the rare earth industry. Consequently, significant research efforts have been directed toward the modeling, control, and optimization of the rare earth extraction process, yielding substantial findings.

Regarding extraction process modeling, a bilinear dynamic model factoring in state lag was established in ref 1, predicated on the multistage dynamic characteristics of rare earth extraction. This model, however, neglects the interaction between stages and subsequently loses certain dynamic traits. In ref 2, the mixer clarifier was approximated as a mixer coupled with a pure hysteresis link, leading to the establishment of a dynamic model of the copper extraction process based on a material balance relationship. Concurrently, an extraction equilibrium relationship between two phases was described by using the extraction balance model. Reference 3 expanded upon ref 2 by providing a more granular depiction of

the clarifier, which brings the model closer to actual extraction processes. In ref 4, a dynamic model of the rare earth extraction process was proposed based on the principle of stepwise extraction, and the system’s dynamic and static characteristics were thoroughly analyzed. Reference 5 modeled the multicomponent separation process of rare earth extraction by solving a vast array of nonlinear equations. Some researchers have employed data-driven methodologies such as artificial neural networks<sup>6,7</sup> and multi-RBF neural network models<sup>8</sup> to create rare earth extraction models. Nevertheless, these methods struggle to accurately represent the extensive dynamic process of rare earth extraction. Upon review of the preceding analysis, a conspicuous absence of a state space model based on the mechanism of rare earth extraction is evident.

**Received:** September 18, 2023

**Revised:** October 9, 2023

**Accepted:** October 12, 2023

**Published:** October 26, 2023



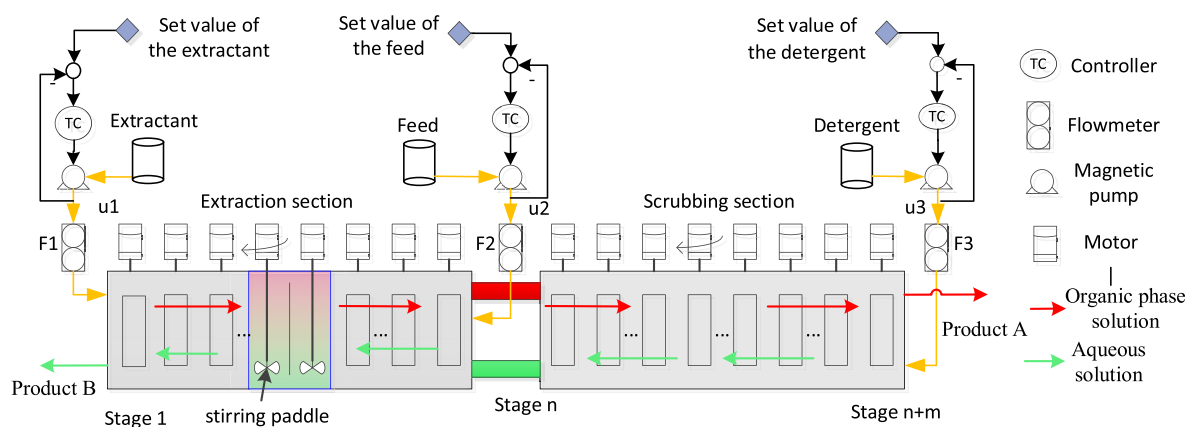


Figure 1. Rare earth extraction process description.

For drug dosage control within the rare earth extraction process, the current industrial practice revolves around “offline analysis, manual adjustment, and experience control”.<sup>9,10</sup> An optimization control system for the rare earth extraction process, predicated on two-layer architecture and case-based reasoning technology, was proposed in ref 11. However, only case-based reasoning technology was utilized in its optimization layer. A control method fusing static setting with dynamic compensation was introduced in ref 12, showcasing promising results in experimental settings, albeit with stringent requirements on industrial data. A novel multimodel switching predictive control scheme was proposed in ref 13 premised on the development of a multi-input and multioutput local linear model. Nevertheless, this scheme failed to discuss the stability of the model switching. In ref 14, a control method for component content distribution in the rare earth extraction process was proposed, wherein a progressive step model is established according to each stage and the control target is achieved by dynamically adjusting the extractant and detergent flow. Taking into consideration the characteristic that the content of rare earth elements merely needs to be confined within a certain range, ref 15 proposed a combination of an interval control strategy and a generalized predictive control algorithm, employing different control intensities and strategies for varying system operating conditions. In ref 16, PID controllers were designed for distinct specific operating conditions to implement distributed control of the extraction system. However, the sole utilization of PID exhibits limitations for a demanding production process. The extraction mechanism analysis of the generalized predictive control method, in conjunction with the dynamic characteristics of the rare earth extraction process, was discussed in ref 17.

At present, the dosage of the rare earth extraction drug is still manually controlled, leading to difficulties in adjusting the inlet flow in a timely and accurate manner when production conditions vary. This often results in the rare earth production index falling short of the requirements. Thus, given that model predictive control<sup>18,19</sup> can surmount the variation of rare earth extraction conditions<sup>20</sup> to enhance the system’s anti-interference ability, this paper employs this method in lieu of manual control of drug dosage, considering the perspective of the rare earth extraction mechanism. Model predictive control is widely criticized for its frequent online timing sampling communication and substantial computational requirements. However, when the process index error is negligible and does not compromise product quality, the event trigger determines

whether to update the controller based on the current state of the system, effectively reducing the frequency of controller updates.<sup>21,22</sup> In ref 23, the event-triggered control was employed in the equilibrium point temperature control of a continuous stirred tank reactor (CSTR), improving the system’s robustness and significantly saving energy. The fuzzy control method of the event-triggering mechanism was proposed and applied to the temperature control of a zinc baking furnace in ref 24, drastically decreasing controller execution and mitigating actuator wear. In ref 25, an event-triggering mechanism was designed as a control increment threshold to efficiently reduce the number of controller updates.

In summary, this paper proposes and applies a constrained model predictive control method for rare earth extraction, predicated on an event-triggering mechanism, to the flow control of extractants and detergents in the rare earth extraction process. The first step involves a comprehensive analysis of the characteristics of the rare earth extraction mechanism, culminating in the derivation of a linear state space model. Second, in light of the input and output constraints inherent in the extraction process and the explicit constraint handling capability of predictive control,<sup>26</sup> an objective optimization function featuring input and output constraints is established. Subsequently, to swiftly counteract the secondary disturbances of the extractant and detergent flow, cascade control<sup>27</sup> is utilized to enhance flow control precision. Moreover, in consideration of the varying impact of different mining conditions on the weight of its objective optimization function, a fuzzy method<sup>28</sup> is employed to adjust the output error weight matrix of its objective optimization function. Finally, a fixed-threshold event-triggering mechanism is designed to effectively alleviate the execution burden on the controller.

## PROCESS DESCRIPTION AND CONTROL SCHEME ANALYSIS

**Process Description.** The current practices in the rare earth industry predominantly employ a method known as cascade fractionation for extraction. This process involves repeated interaction of the aqueous phase with the organic phase, facilitating the separation and extraction of individual rare earth elements of the desired purity from a composite rare earth solution. Referring to Figure 1, let us assume the feed liquid to be an organic phase feed. The comprehensive rare earth extraction production line is composed of an  $n$ -stage

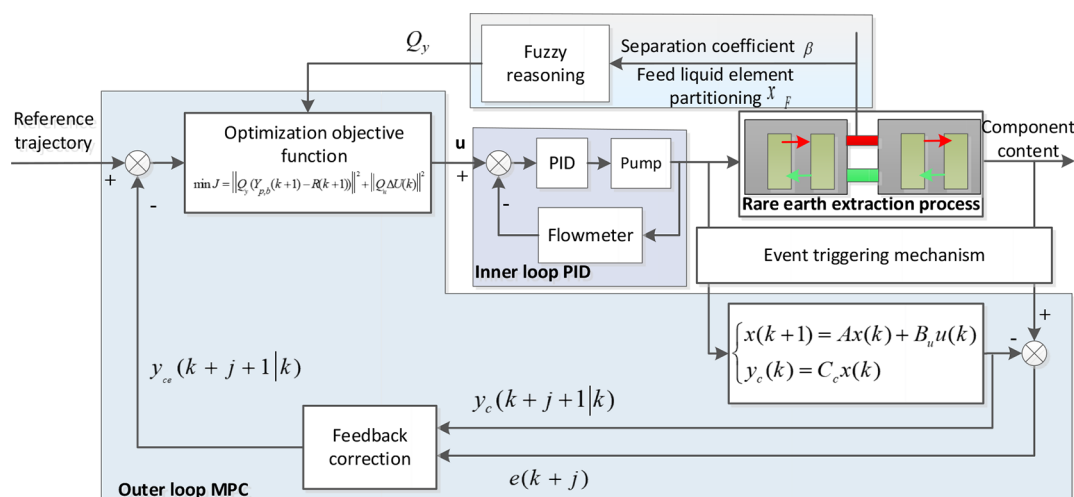


**Figure 2.** Constrained model predictive control scheme for the rare earth extraction process based on event triggering.

extraction section followed by an  $m$ -stage washing section, cumulatively consisting of  $n + m$  extraction tanks. The solution situated beneath each stage of the extraction tank is categorized as the aqueous phase, while the solution above is delineated as the organic phase. During the operational procedure, extractant  $u_1$  is introduced into the first stage of the extraction tank. Subsequently, material liquid  $u_2$  is infused into the  $n$ -stage extraction tank, while detergent  $u_3$  is incorporated into the  $n + m$  stage extraction tank. Due to the distinctive architectural design of the extraction tanks coupled with the impact of the stirring force, the organic phase is observed to flow from left to right. Conversely, the aqueous phase demonstrates a flow from right to left within all levels of the extraction tank. As a result of the interplay between the extractants and detergents, the rare earth solution undergoes a step-by-step extraction. In conclusion, the aqueous phase exit of the initial stage in the extraction section yields a product, B, which is challenging to extract. Conversely, the organic phase exit of the  $n + m$  stage in the washing section procures product A, which exhibits a more straightforward extraction profile.

In the rare earth extraction procedure, the flow rate of the feed liquid is contingent on the daily throughput stipulated by the production plan. Given a constant processing capacity, the feed liquid flow usually remains unaltered. However, it can experience minor fluctuations due to the influence of the transportation pump. The primary objective of the rare earth extraction process is to calibrate the flow rates of the extractant and detergent in such a manner that the purity of the easily extractable product A from the organic phase and the difficult-to-extract product B from the aqueous phase both adhere to the stipulated production standards.

On the industrial floor, technicians determine the flow rates for both the extractant and detergent based on empirical testing outcomes. Once these rates are initially established by the operator, drawing on prior experience, they can be fine-tuned using PID technology, acting as an inner loop, as illustrated in Figure 1. Because the rare earth extraction process is a complex industrial process, the production operation mode is seriously lagging behind, and when the operating conditions change, the rare earth extraction production process needs a long time to stabilize.

**Control Scheme Analysis.** The inner loop of the proposed control system is regulated by PID, while the outer

loop is controlled by the model predictive control method, which supersedes manual adjustments of the extractant and detergent flow. Furthermore, based on the variance of process indicators within a specified range, an event-triggering mechanism is utilized to reduce the frequency of communication and actuator execution. The control scheme, illustrated in Figure 2, encompasses various modules including a trigger mechanism, outer loop model predictive control, inner loop PID control, and fuzzy reasoning. The process begins with the derivation of the prediction model for rare earth extraction. To account for any discrepancies between the model and the actual rare earth extraction process, a correction link is implemented. Subsequently, the optimal objective function with input and output constraints is established. The output error weight matrix is set by employing a fuzzy reasoning method, in accordance with the separation coefficient and raw material allocation under ore entry conditions. The optimization problem is then resolved to obtain the extractant and detergent flow values that align with real-time operating conditions, with subsequent control of these values being facilitated by a PID controller.

Lastly, given that the content of rare earth components lies within a reasonable range, it becomes unnecessary to further adjust the drug dosage. Based on this observation, an event-triggering mechanism is introduced to assess whether any component content within the monitored process level surpasses the allowed range, thus determining whether controller implementation is necessary.

## ■ CONSTRAINED MODEL PREDICTIVE CONTROL OF THE RARE EARTH EXTRACTION PROCESS BASED ON EVENT TRIGGERING

**State Space Model for the Rare Earth Extraction Process.** The production process of two-component rare earth extraction in a rare earth production enterprise is taken as the object, and the stages of extraction and washing are respectively  $n = 13$  and  $m = 9$ . According to its industrial production data, the feed liquid composition is  $f_a = 0.47$  and  $f_b = 0.52$ , respectively, so the ratio of raw materials is  $x_F = 1.1$ . The cumulative totals of the aqueous phase and organic phase in the tank are 14.7 and 2.6 L, respectively. The inlet flow rates of the extractant, feed, and detergent are  $u_1 = 9.1$  L/min,  $u_2 = 1$  L/min, and  $u_3 = 1.9$  L/min, respectively. With the

concentration of each rare earth element in each aqueous phase and organic phase as the state quantity, it is assumed that  $x_A(k)$  and  $x_O(k)$  represent the concentrations of the difficult extraction element in each aqueous phase and the easy extraction element in each organic phase, respectively. Taking the content of rare earth elements in difficult and easy extraction as the output, it is assumed that  $Y_{1,1}$  is the purity of difficult extraction elements in the first stage and  $Y_{2,n+m}$  is the purity of easy extraction elements in the  $n + m$  stage. According to the extraction theory,<sup>29,30</sup> the state space model of extraction is as follows.

$$\begin{cases} x(k+1) = Ax(k) + B_u u(k) \\ y_c(k) = C_c x(k) \end{cases} \quad (1)$$

where  $x(k) = (x_A(k) \ x_O(k))^T$ ,  $y_c(k) = (Y_{1,1}(k) \ Y_{2,n+m}(k))^T$ , state matrix

$$A_1 = \begin{pmatrix} A_1 & O \\ O & A_2 \end{pmatrix} = \begin{bmatrix} -12.88 & 12.88 & \cdots & 0 & 0 & \cdots & 0 \\ \vdots & \vdots & \vdots & \vdots & \vdots & \vdots & \vdots \\ 0 & \cdots & -12.88 & 12.88 & 0 & \cdots & 0 \\ \vdots & \vdots & \vdots & \vdots & -2.85 & 2.85 & \vdots \\ 0 & \cdots & \vdots & \vdots & \vdots & \vdots & 2.85 \\ \vdots & \vdots & \vdots & \vdots & \vdots & \vdots & \vdots \\ 0 & \cdots & \vdots & 0 & 0 & \cdots & -2.85 \end{bmatrix}_{22 \times 22}$$

$$A_2 = \begin{bmatrix} -14.74 & \cdots & \cdots & \cdots & \cdots & 0 \\ 14.74 & -14.74 & \cdots & \cdots & \cdots & \vdots \\ 0 & 14.74 & \cdots & \cdots & \cdots & \vdots \\ \vdots & \vdots & \vdots & \vdots & \vdots & \vdots \\ \vdots & \vdots & \vdots & \vdots & \vdots & \vdots \\ 0 & \cdots & \cdots & 0 & 14.74 & -14.74 \end{bmatrix}_{22 \times 22}$$

input matrix  $B_u = (B_1 \ B_2)^T$ ,

$$B_1 = \begin{bmatrix} 0 & 0 & 0 \\ \vdots & \vdots & \vdots \\ 0 & 0.78 & \vdots \\ \vdots & \vdots & \vdots \\ 0 & 0 & 0.18 \end{bmatrix}_{22 \times 3}$$

$$B_2 = \begin{bmatrix} 0.11 & 0 & 0 \\ 0 & 0 & 0 \\ \vdots & \vdots & \vdots \\ 0 & 0.84 & 0 \\ \vdots & \vdots & \vdots \\ 0 & 0 & 0 \end{bmatrix}_{22 \times 3}$$

and the output matrix

$$C_c = \begin{bmatrix} 1 & 0 & \cdots & 0 \\ 0 & \cdots & 0 & 1 \end{bmatrix}_{2 \times 44}$$

Then, the state space increment model of the linear discrete real-time system is as follows.

$$\begin{cases} \Delta x(k+1) = A\Delta x(k) + B_u \Delta u(k) \\ y_c(k) = C_c \Delta x(k) + y_c(k-1) \end{cases} \quad (2)$$

where  $\Delta x(k) = x(k) - x(k-1)$ ,  $\Delta u(k) = u(k) - u(k-1)$ ,  $\Delta x(k)$  is the state increment,  $\Delta u(k)$  is the control input increment, and  $y_c(k)$  is the controlled output.

**Model Predictive Control with Input and Output Constraints.** Assuming that  $p$  and  $m$  represent the prediction horizon and control horizon, respectively, the derivation of the control law necessitates the computation of the predicted state for future  $p$  steps pertaining to the content of rare earth elements. Following this, the predicted output is procured through feedback correction and substitution of the objective

function. Subsequently, the constrained optimization problem is reformulated into a quadratic programming form, ultimately yielding the requisite drug dosage.

According to eq 2, the state increment of step  $k + 1$  is as follows.

$$\Delta x(k+1) = A\Delta x(k) + B_u \Delta u(k) \quad (3)$$

The state increment of step  $k + m$  is obtained by iteration:

$$\begin{aligned} \Delta x(k+m) &= A^m \Delta x + A^{m-1} B_u \Delta u(k) \\ &\quad + A^{m-2} B_u \Delta u(k+1) + \cdots \\ &\quad + B_u \Delta u(k+m-1) \end{aligned} \quad (4)$$

Then, the state increment of step  $k + p$  is as follows:

$$\begin{aligned} \Delta x(k+p) &= A^p \Delta x + A^{p-1} B_u \Delta u(k) \\ &\quad + A^{p-2} B_u \Delta u(k+1) + \cdots \\ &\quad + A^{p-m} B_u \Delta u(k+m-1) \end{aligned} \quad (5)$$

Calculate the forecast output from  $k + 1$  to  $k + p$  based on the forecast state. According to eq 2, the predicted output of step  $k + 1$  is

$$y_c(k+1) = C_c A \Delta x(k) + C_c B_u \Delta u(k) + y_c(k) \quad (6)$$

Get the predicted output of step  $k + m$  by iterating:

$$\begin{aligned} y_c(k+m) &= C_c \Delta x(k+m) + y_c(k+m-1) \\ &= \sum_{i=1}^m C_c A^i \Delta x(k) + \sum_{i=1}^{m-1} C_c A^{i-1} B_u \Delta u(k) + \cdots \\ &\quad + C_c B_u \Delta u(k+m-1) + y_c(k) \end{aligned} \quad (7)$$

Then, the predicted output of step  $k + p$  is as follows:

$$\begin{aligned} y_c(k+p) &= C_c \Delta x(k+p) + y_c(k+p-1) \\ &= \sum_{i=1}^p C_c A^i \Delta x(k) + \sum_{i=1}^{p-1} C_c A^{i-1} B_u \Delta u(k) \\ &\quad + \sum_{i=1}^{p-1} C_c A^{i-1} B_u \Delta u(k+1) + \cdots \\ &\quad + \sum_{i=1}^{p-m+1} C_c A^{i-1} B_u \Delta u(k+m-1) + y_c(k) \end{aligned} \quad (8)$$

In order to improve the accuracy of the model, by calculating the error  $e(k+j)$  between the actual output in the production process of step  $k + j$ ,  $j \in [0, p-1]$ , and the output value predicted by the model, the feedback correction results in the predicted output value of step  $k + j + 1$  as follows:

$$y_{ce}(k+j+1) = y_c(k+j+1) + e(k+j) \quad (9)$$

Considering the characteristics of the rare earth extraction production process, the input (feed, extractants, and detergents) and output (element component content) both meet certain constraints. In order to make the output response track the reference trajectory, an optimization objective function with input and output constraints is established:

$$\min J = \sum_{j=1}^{n_y} \sum_{i=1}^p \left\| Q_{i,j}^y (y_{ce}(k + ilk) - r_j(k + i)) \right\|^2 + \sum_{j=1}^{n_u} \sum_{i=1}^m \left\| Q_{i,j}^{\Delta u} \Delta u(k + i - 1) \right\|^2 \tag{10}$$

s.t.  $\Delta x(k + i + 1)k = A\Delta x(k + ilk) + B_u\Delta u(k + i)$ ;  $y_{ce}(k + ilk) = C_c\Delta x(k + ilk) + y_c(k + i - 1)k + e(k + i - 1)$ ;  $u_{\min} = 0 \leq u(k + i) \leq u_{\max} = 80$ ,  $i \in [0, m - 1]$ ;  $y_{\min} = 0 \leq y_{ce}(k + i) \leq y_{\max} = 1$ ,  $i \in [1, p]$ .

where  $r_j(k + 1)$  is the  $j$ th component of the given reference input sequence. Since the input variables are the extractant, feed liquid, and detergent and the output variables are the component content of difficult and easily extracted rare earth elements,  $n_u$  and  $n_y$  are 3 and 2, respectively. The output error weight matrix is  $Q_{y1}^{\text{def}} = \text{diag}\{Q_{1,1}^y, \dots, Q_{p,1}^y\}_{p \times p}$  and  $Q_{y2}^{\text{def}} = \text{diag}\{Q_{1,2}^y, \dots, Q_{p,2}^y\}_{p \times p}$ , respectively.

Since the optimization objective function (eq 10) has constraints, the optimization objective can be transformed into a quadratic programming problem. Then, the optimal control sequence  $\Delta U^*(k)$  is obtained, and the first element of the solution is applied to the controlled system.

**Output Error Weight Matrix Adjustment Based on Fuzzy Inference.** The weighting matrix in eq 10 is generally fixed after adjustment. However, the tracking performance is mainly affected by output error weight matrices  $Q_{y1}$  and  $Q_{y2}$ . Within the rare earth extraction process, elements such as the separation coefficient of the stock liquid, the allocation of raw materials, and other ore entry conditions significantly impact the production index.<sup>31</sup> Different mining conditions correlate with varied operating conditions, hence necessitating distinct dosages for production.<sup>32</sup> In order to adapt to different operating conditions,  $Q_{y1}$ ,  $Q_{y2}$ , and mining conditions can be established as follows:

$$\begin{cases} Q_{y1} = f(\beta, x_F | \psi_1) \\ Q_{y2} = f(\beta, x_F | \psi_2) \end{cases} \tag{11}$$

where  $f(\cdot | \psi)$  represents a fuzzy function whose parameters are  $\psi$  (such as membership function and fuzzy semantic control rules).  $\beta$  and  $x_F$  represent the separation coefficient and the ratio of raw material allocation, respectively.

Based on fuzzy system theory, the parameter  $\psi$  can be written as follows:

$$\begin{cases} \psi_1 = [k_{h1}, k_{g1}, k_{u1}, a_{h1}, b_{h1}, c_{h1}, a_{g1}, b_{g1}, c_{g1}, a_{y1}, b_{y1}, c_{y1}] \\ \psi_2 = [k_{h2}, k_{g2}, k_{u2}, a_{h2}, b_{h2}, c_{h2}, a_{g2}, b_{g2}, c_{g2}, a_{y2}, b_{y2}, c_{y2}] \end{cases} \tag{12}$$

where  $k$  represents the proportion (scale) factor of fuzzy control and subscripts  $h$ ,  $g$ , and  $u$  represent the separation coefficient, the ratio of raw material allocation, and weight, respectively.  $a$ ,  $b$ , and  $c$  represent the set of parameters for the triangular membership function, as shown in Figure 3. When two adjacent membership functions are determined, their

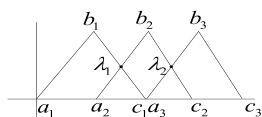


Figure 3. Membership function of the characteristic parameter.

intersection point,  $\lambda$ , is determined. In general, the intersection point  $\lambda$  should be located at the center of the two membership functions, which can respond quickly to the input and accurately to changes in a small range of the input.

The membership function of the characteristic parameters is shown in Figure 3. After establishing the fuzzy rule table, the inverse fuzzy is carried out, the gravity center method is used to deblur the fuzzy output, and the corrected output weight is finally obtained.

**Event-Triggering Mechanism.** In a conventional time-triggered MPC, measurement signals are sampled at consistent intervals, and control signals undergo periodic updates. This process often results in an overabundance of sampling and control operations. In contrast, event-triggered control functions according to specific predefined conditions initiate controller updates solely when these criteria are satisfied. Consequently, event-triggered control significantly reduces the frequency of controller and actuator operations, alleviating computational and communication burdens.

As depicted in Figure 1, the contents of the hard-to-extract "B" elements and easy-to-extract "A" elements in the rare earth extraction process are confined within certain reasonable index ranges. When the error between the actual and given values of the component content at an outlet exceeds a certain threshold, the controller is required to compute the current dosage to manage the production condition. Thus, the triggering mechanism can be articulated in set notation as follows:

$$\Theta = \{k_s | \|r_i(k_s) - y_i(k_s)\| \geq e_{\text{opti}}\} \tag{13}$$

where  $k_s$  indicates the controller trigger time,  $r_i(k_s)$  is the set value for the content of element  $i$ ,  $y_i(k_s)$  is the content of element  $i$ , and  $e_{\text{opti}} > 0$  is the threshold of component content error.

## SUMULATION RESULTS AND ANALYSIS

**Parameter Setting.** The control parameters are obtained by cross verification in the simulation. For a predictive

Table 1.  $Q_{y1}$  Membership Function Value of Characteristic Parameters

no.	separation coefficient			the ratio of raw material allocation			$Q_{y1}$		
	$a_{h1}$	$b_{h1}$	$c_{h1}$	$a_{g1}$	$b_{g1}$	$c_{g1}$	$a_{y1}$	$b_{y1}$	$c_{y1}$
1	1	2	3	0.25	0.5	0.75	1.4	1.4	0.9
2	2	3	4	0.5	0.75	1	1.4	0.9	0.5
3	3	4	5	0.75	1	1.25	0.9	0.5	0.9
4	4	5	6	1	1.25	1.5	0.5	0.9	0.9
5	5	6	7	1.25	1.5	1.75	0.9	0.9	0.9

Table 2.  $Q_{y2}$  Membership Function Value of Characteristic Parameters

no.	separation coefficient			the ratio of raw material allocation			$Q_{y2}$		
	$a_{h1}$	$b_{h1}$	$c_{h1}$	$a_{g1}$	$b_{g1}$	$c_{g1}$	$a_{y2}$	$b_{y2}$	$c_{y2}$
1	1	2	3	0.25	0.5	0.75	1.6	1.6	1.1
2	2	3	4	0.5	0.75	1	1.6	1.1	0.6
3	3	4	5	0.75	1	1.25	1.1	0.6	0.4
4	4	5	6	1	1.25	1.5	0.6	0.4	0.3
5	5	6	7	1.25	1.5	1.75	0.4	0.3	0.3

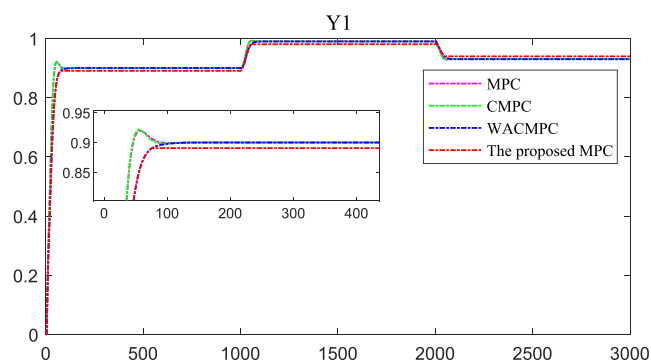
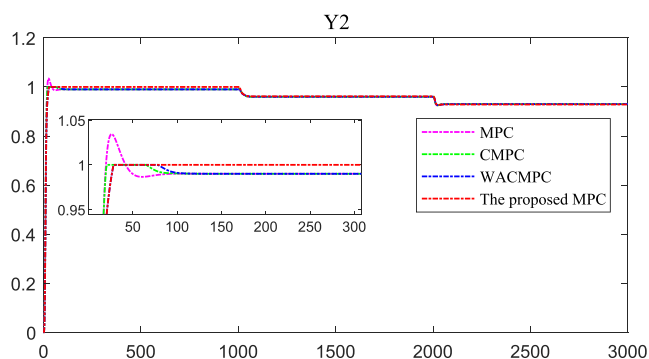
(a)  $Y_1$  response curve(b)  $Y_2$  response curve

Figure 4. Simulation results of operating condition 1.

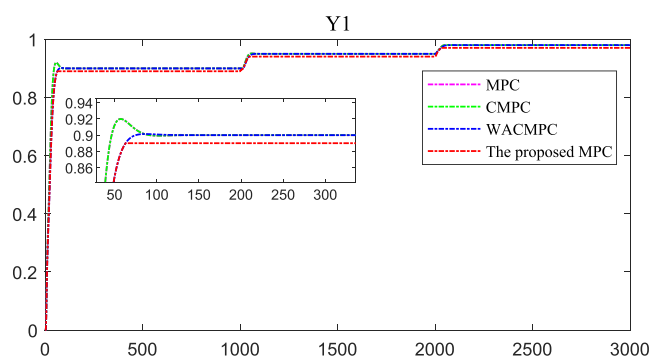
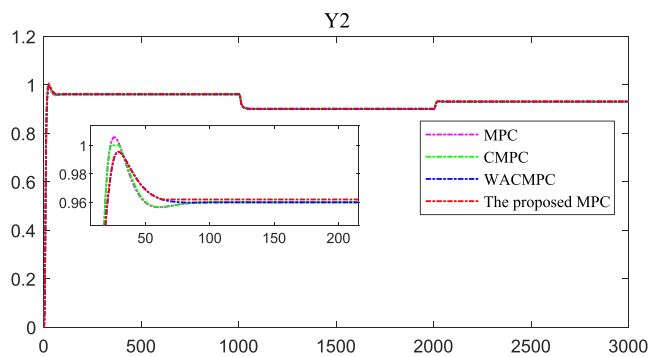
(a)  $Y_1$  response curve(b)  $Y_2$  response curve

Figure 5. Simulation results of operating condition 2.

controller,  $p = 10$ ,  $m = 2$ , and  $Q_u = \text{diag}(0.03, 0.08, 0.03)$ . For the fuzzy inference module, the value of the feature parameter

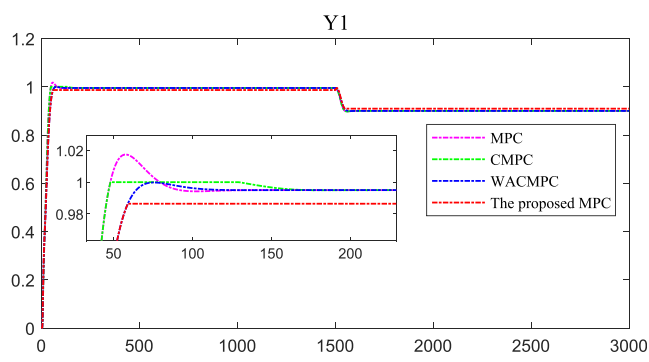
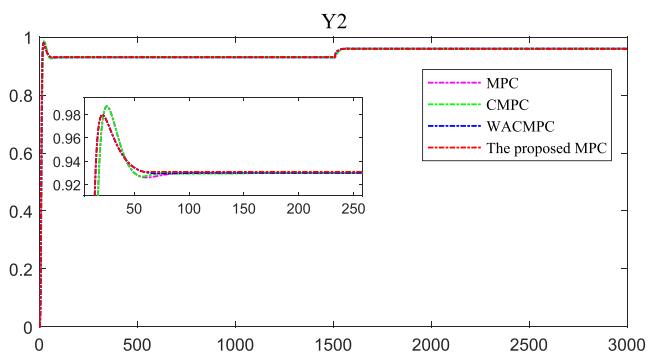
(a)  $Y_1$  response curve(b)  $Y_2$  response curve

Figure 6. Simulation results of operating condition 3.

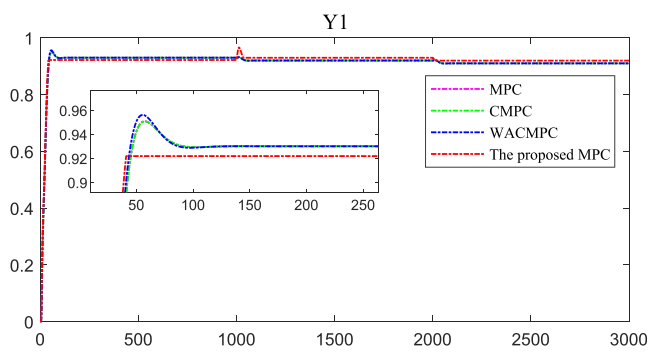
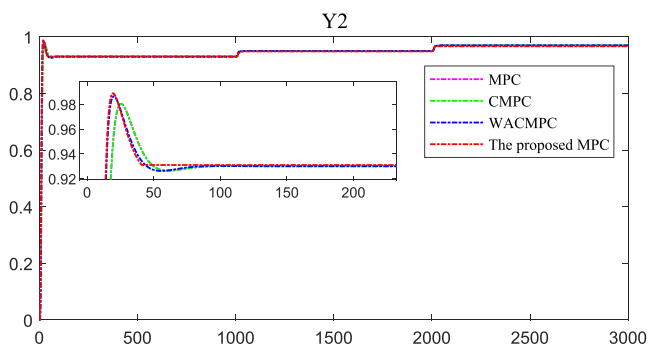
(a)  $Y_1$  response curve(b)  $Y_2$  response curve

Figure 7. Simulation results of operating condition 4.

$\psi$  is determined. According to the process test and expert experience, the separation coefficient theoretically spans from 1 to 7, with an established value of 4. Similarly, the theoretical range for the ratio of raw material allocation is between 0.25

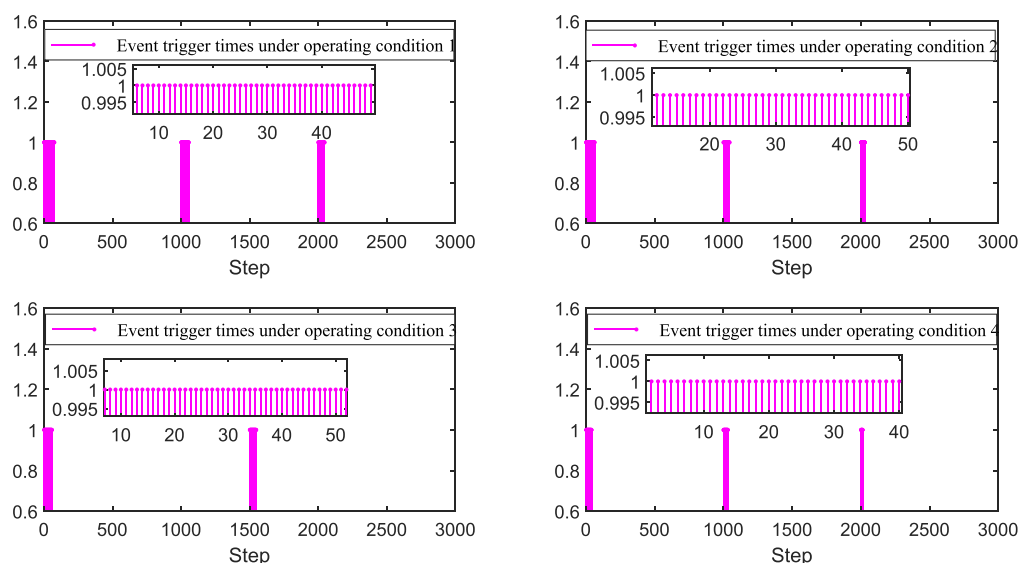


Figure 8. Events triggered under different operating conditions.

Table 3. Performance Comparison of Different Control Methods

cost	MPC	CMPC	WACMPC	the proposed method
operating condition 1	216,211	215,460	213,965	214,883
operating condition 2	205,026	205,030	204,033	204,335
operating condition 3	209,768	209,739	204,750	204,355
operating condition 4	215,312	215,312	210,402	207,564

Table 4. Control Performance and Trigger Analysis of Different Operating Conditions

operating condition	performance deterioration rate	number of triggers	trigger reduction rate
operating condition 1	0.43%	175	94.17%
operating condition 2	0.15%	136	95.47%
operating condition 3	−0.19%	105	96.50%
operating condition 4	−1.3%	85	97.17%

and 1.75, with a set value of 1. The distinct parameter values for the output error weight matrices  $Q_{y1}$  and  $Q_{y2}$  are detailed in Tables 1 and 2, respectively.

**Analysis of Comparative Methods.** To demonstrate the efficacy of our proposed method, we compared it with three other techniques. These are method 1, which utilizes unconstrained predictive control (MPC); method 2, which employs constrained predictive control (CMPC); and method 3, which is based on the weight-adaptive constraint predictive control (WACMPC). Our proposed approach is characterized as method 4: the event-triggering constraint model predictive control method, and the trigger threshold is  $e_{opt1} = e_{opt2} = 0.01$ . The output error weight matrix for methods 1 and 2 is  $Q_y = \text{diag}(1,1)$ . The output error weight matrix  $Q_y = \text{diag}(Q_{y1}, Q_{y2})$  of methods 3 and 4 is obtained by fuzzy reasoning.

In the rare earth extraction process, the separation coefficient of the stock liquid and the ratio of raw material allocation have a great impact on the production index. These two parameters directly depict the prevailing operating conditions. This paper examines the performance of control algorithms under four distinct operating scenarios representative of varied production processes: The first scenario is characterized by a low separation coefficient and a high ratio of the raw material allocation. In the second scenario, there is an excessively large separation coefficient paired with a markedly small ratio of raw material allocation. The third scenario presents a condition where both the separation coefficient and the ratio of raw material allocation are significantly large. The fourth and final operating condition involves a small separation coefficient coupled with a low ratio of the raw material allocation.

(1) Typical operating conditions in condition 1:  $\beta = 1.7$  and  $x_F = 1.1$ .  $Y_1$  is the component content of the hardly extracted product, while  $Y_2$  is the component content of the easily extracted product. The simulation results of component contents  $Y_1$  and  $Y_2$  are shown in Figure 4. It can be seen from Figure 4 that all four control algorithms can make the content of rare earth components track the target value, but the control algorithm proposed in this article realizes a smaller overshoot and can quickly reach the target interval. Referring to Figure 4b, it is evident that, in contrast to unconstrained MPC, the other three algorithms satisfy the production constraints. This observation underscores the notable benefits of constrained model predictive control algorithms when applied to real-world production systems. Moreover, a review of the simulation outcomes reveals that systems with optimized weights exhibit enhanced stability in their dynamic responses, resulting in diminished fluctuations in system output.

(2) Typical operating conditions 2:  $\beta = 4.1$  and  $x_F = 0.5$ . The simulation results of component contents  $Y_1$  and  $Y_2$  are shown in Figure 5. As can be seen from Figure 5, the tracking error of the proposed method is within 0.01, which meets the reasonable range of rare earth element production. Methods 3 and 4 use fuzzy inference modules to achieve faster tracking and smaller fluctuations. According to Figure 5b, CMPC can make the content of rare earth components meet the constraint

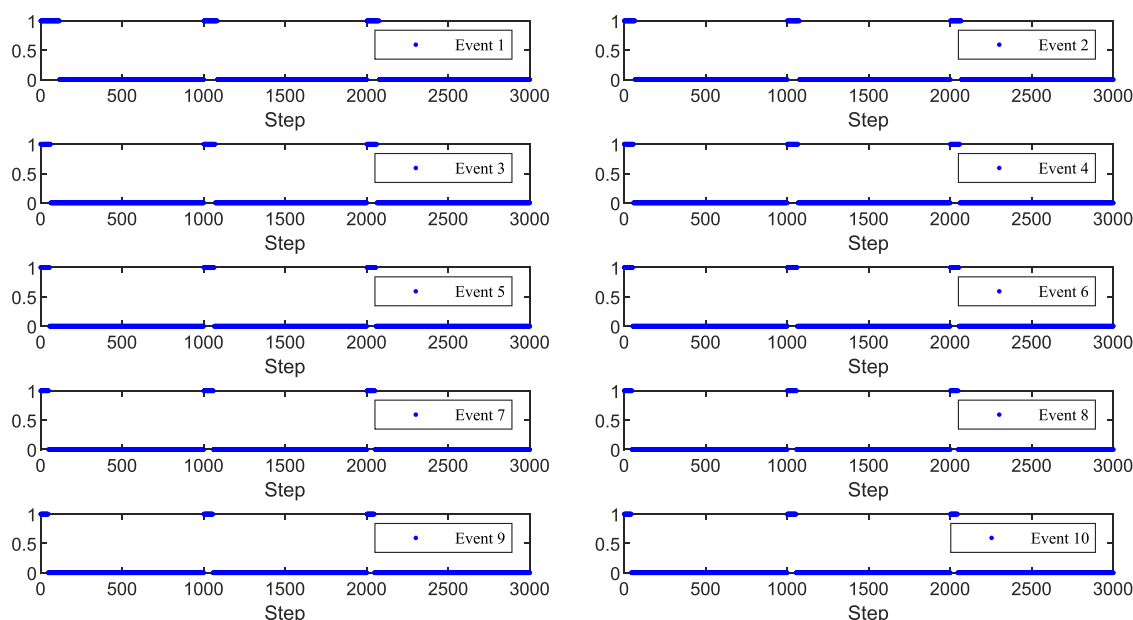


**Figure 9.** Triggers of events with different thresholds.

conditions well, while method 1 is not in line with the actual situation because the output component content is greater than 1 due to no constraint.

(3) Typical operating conditions 3:  $\beta = 5$  and  $x_F = 1.8$ . The simulation results of component contents  $Y_1$  and  $Y_2$  are shown in Figure 6. According to Figure 6, compared with MPC, CMPC, and WACMPC, the method proposed in this paper has a smaller overshoot and less dynamic process fluctuation. In this paper, the event-triggering mechanism is added to make the system tracking more smooth, and the component content of export products can be within the set range of 0.01.

(4) Typical operating conditions 4:  $\beta = 3.1$  and  $x_F = 0.5$ . The simulation results of component contents  $Y_1$  and  $Y_2$  are shown in Figure 7. As can be seen from Figure 7, compared with unconstrained MPC, CMPC, and WACMPC, the MPC algorithm proposed in this paper can accurately track the target value and achieve stability quickly, thus reducing the adjustment time when the disturbance occurs.

As shown in Figures 4–7, the proposed method can meet both production output constraints and threshold requirements to ensure a better control effect. Moreover, compared with the nonevent-triggered method, the steady-state process has no fluctuation and runs very smoothly.

**Impact of the Triggering Mechanism on System Performance.** Figure 8 delineates the event-triggering conditions under the four distinct operating scenarios discussed in the previous section. From the figure, it is evident that the frequency of event triggers fluctuates based on the operating conditions. In some instances, triggers occur only briefly, with the system predominantly maintaining a non-trigger state. Such triggering predominantly transpires during the system's dynamic phase when the disparity between its actual and set values surpasses the designated threshold. Conversely, as the system transitions into a steady state, the steady-state error remains below the threshold, meaning that trigger conditions are unmet, and consequently, there is no need for controller updates.

Table 3 presents the consumption data for the extractant flow and detergent flow across the four methods. This metric

serves as a viable indicator of control efficacy: a reduced consumption signifies superior control performance. Observing Table 3, it becomes evident that, while the proposed method's effectiveness lags behind that of WACMPC under operating conditions 1 and 2, it still outperforms both MPC and CMPC. Table 4, on the other hand, details the event-triggering conditions and control costs associated with the proposed method across varying operational scenarios. As inferred from Table 4, while the integration of event triggers may slightly compromise the control performance, this degradation is marginal, not exceeding 2%. Notably, there is a reduction of over 90% in the frequency of event triggers, which substantially alleviates the controller's computational demands.

In the simulation experiment detailed in the previous section, the threshold emerges as a critical parameter for the controller, profoundly influencing both control performance and the frequency of controller updates. To elucidate this relationship, this paper scrutinizes the system's control behavior across various threshold scenarios. The event-triggering scenarios are visualized in Figure 9, where events labeled from 1 to 10 correspond to 10 distinct thresholds spanning from 0.001 to 0.01. An examination of Figure 9 reveals that the selection of thresholds dictates the event-triggering patterns with an upward trend in the threshold resulting in fewer triggers.

In summation, the proposed methodology not only enhances both dynamic and static response processes of the system but also ensures that the rare earth component's content precisely aligns with the predefined set values. Concurrently, it significantly alleviates the computational demands placed on the controller.

## CONCLUSIONS

Given the dearth of available state space models specific to rare earth extraction for reference, this work innovatively proposes a rare earth extraction state space model. Recognizing the flexibility within which the rare earth component content can operate during the production phase, a constrained model predictive control method for the rare earth extraction

component content, underpinned by an event-triggering mechanism, is proposed herein. Finally, the control performance of the system under different typical operating conditions is tested, which shows the effectiveness of the proposed method. These findings pave the way for future explorations, such as using the mechanism and data driven to increase the accuracy of the model and distributed predictive control technology to deal with the multicomponent rare earth extraction process.

## AUTHOR INFORMATION

### Corresponding Author

Jianyong Zhu – School of Electrical and Automation Engineering, East China Jiaotong University, Nanchang, Jiangxi 330013, P.R. China; Email: [zhujyemail@163.com](mailto:zhujyemail@163.com)

### Authors

Zhiyong Zhang – School of Electrical and Automation Engineering, East China Jiaotong University, Nanchang, Jiangxi 330013, P.R. China; [orcid.org/0009-0001-0952-4471](https://orcid.org/0009-0001-0952-4471)

Cong Xiong – School of Electrical and Automation Engineering, East China Jiaotong University, Nanchang, Jiangxi 330013, P.R. China

Hui Yang – School of Electrical and Automation Engineering, East China Jiaotong University, Nanchang, Jiangxi 330013, P.R. China

Feiping Nie – School of Artificial Intelligence, Optics and Electronics (iOPEN), Northwestern Polytechnical University, Xi'an 710072, P.R. China

Complete contact information is available at:  
<https://pubs.acs.org/10.1021/acsomega.3c07153>

### Notes

The authors declare no competing financial interest.

## ACKNOWLEDGMENTS

The work was supported by the National Key Research and Development Program (no. 2020YFB1713700), the National Natural Science Foundation of China (nos. 62363010 and 61963015), the Jiangxi Double Thousand Plan (no. SSQ2023018), and the Science and Technology Research Project of Education Department of Jiangxi Province (no. GJJ191424).

## REFERENCES

- (1) Jia, W. J.; Chai, T. Y. Bilinear model of rare earth cascade extraction process and its parameter identification. *Control Theory Appl.* **2006**, *23* (5), 717–723.
- (2) Komulainen, T.; Pekkala, P.; Rantala, A.; Jamsa-Jounela, S. L. Dynamic modelling of an industrial copper solvent extraction process. *Hydrometallurgy* **2006**, *81* (1), 52–61.
- (3) Moreno, C. M.; Pérez-Correa, J. R.; Otero, A. Dynamic modelling of copper solvent extraction mixer-settler units. *Miner. Eng.* **2009**, *22* (15), 1350–1358.
- (4) Wiehterlova, J.; Rod, V. Dynamic behavior of the mixer-settler cascade. Extractive separation of the rare earths. *Chem. Eng. Sci.* **1999**, *54* (18), 4041–4051.
- (5) Yun, C. Y.; Lee, C.; Lee, G. G.; Jo, S.; Sung, S. W. Modeling and simulation of multicomponent solvent extraction processes to purify rare earth metals. *Hydrometallurgy* **2016**, *159*, 40–45.
- (6) Giles, A. E.; Aldrich, C.; Van, J. S. J. Modelling of rare earth solvent extraction with artificial neural nets. *Hydrometallurgy* **1996**, *43* (3), 241–255.
- (7) Anitha, M.; Singh, H. Artificial neural network simulation of rare earths solvent extraction equilibrium data. *Desalination* **2008**, *232* (1–3), 59–70.
- (8) Lu, R.; Ye, Z.; Yang, H.; He, F. Multi-RBF models based prediction of component content for Pr/Nd extraction process. *CIESC J.* **2016**, *67* (3), 974–981.
- (9) Liao, C.; Cheng, F.; Wu, S.; Yan, C. Review and Recent Progresses on Theory of Countercurrent Extraction. *J. Chin. Soc. Rare Earths* **2017**, *35* (1), 1–8.
- (10) Jia, J. T.; Yan, C. H.; Liao, C. S.; Wu, S.; Wang, M. W.; Li, B. G. Automation system in rare earths countercurrent extraction processes. *J. Rare Earths* **2001**, *19* (1), 6–10.
- (11) Chai, T. Y.; Yang, H. Integrated automation system for rare earth counter current extraction process. *J. Rare Earths* **2004**, *22* (6), 752–758.
- (12) Zhu, J. Y.; Yang, H.; Lu, R. X.; Xu, F. P.; Yu, Y. J. Static Setting and Dynamic Compensation Based Optimal Control for the Flow Rate of the Reagent in CePr/Nd Extraction Process. *Acta Autom. Sin.* **2019**, *45* (6), 1186–1197.
- (13) Yang, H.; He, L.; Zhang, Z.; Lu, R.; Tan, C. Multiple-model predictive control for component content of Ce Pr/Nd counter current extraction process. *Inf. Sci.* **2016**, *360*, 244–255.
- (14) Yang, H.; Zhu, F.; Lu, R. X.; Zhang, Z. Y. ANFIS model-based predictive control for Pr/Nd cascade extraction process. *CIESC J.* **2016**, *67* (3), 982–990.
- (15) Lu, R.; He, L.; Yang, H.; Zhang, G. Component content control with zone control for rare earth extraction process. *CIESC J.* **2017**, *68* (3), 1058–1064.
- (16) Yang, H.; Xu, F.; Lu, R.; Ding, Y. Component content distribution profile control in rare earth Counter current extraction process. *Chin. J. Chem. Eng.* **2015**, *23* (1), 192–198.
- (17) Lu, R.; Chen, H.; Yang, H.; Zhu, J. Optimal Control of Rare Earth Extraction Process Based on Bilinear Model. *Control Eng. of China* **2022**, *29* (10), 1736–1742.
- (18) Sanborn, S. D.; Varshney, D.; McAuley, K. B. Orthogonalization-Based Gain Conditioning for Linear Model Predictive Control. *Ind. Eng. Chem. Res.* **2023**, *62*, 1463–1479.
- (19) Liu, S.; Liu, C.; Huang, Y.; Zhao, H. Model Predictive Two-Target Current Control for OW-PMSM. *IEEE Trans. Power Electron.* **2021**, *36* (3), 3224–3235.
- (20) Wu, J.; Wang, Z.; Zhang, L. Unbiased-Estimation-Based and Computation-Efficient Adaptive MPC For Four-Wheel-Independently-Actuated Electric Vehicles. *Mech. Mach. Theory* **2020**, *154*, 10410.
- (21) Li, B.; Xia, J.; Zhang, H.; Shen, H.; Wang, Z. Event-triggered adaptive fuzzy tracking control for stochastic nonlinear systems. *J. Franklin Inst.* **2020**, *357* (14), 9505–9522.
- (22) Huang, Y.; Liu, Y. Practical tracking via adaptive event-triggered feedback for uncertain nonlinear systems. *IEEE Trans. Autom. Control* **2019**, *64* (9), 3920–3927.
- (23) Sinha, A.; Mishra, R. K. Control of a nonlinear continuous stirred tank reactor via event triggered sliding modes. *Chem. Eng. Sci.* **2018**, *187*, 52–59.
- (24) Feng, Z.; Li, Y.; Sun, B.; Yang, C.; Zhu, H.; Chen, Z. A trend-based event-triggering fuzzy controller for the stabilizing control of a large-scale zinc roaster. *J. Process Control* **2021**, *97*, 59–71.
- (25) He, H. J.; Meng, X.; Tang, J.; Qiao, J. F. ET-RBF-PID-based control method for furnace temperature of municipal waste incineration process. *Control Theory Appl.* **2022**, *39* (12), 2262–2273.
- (26) Xi, Y. G.; Li, D. W.; Lin, S. Model Predictive Control — Status and Challenges. *Acta Autom. Sin.* **2013**, *39* (3), 222–236.
- (27) Qian, X.; Huang, K.; Jia, S.; Chen, H.; Yuan, Y.; Zhang, L.; Wang, S. Composition-Temperature Cascade Control of Dividing-Wall Distillation Columns by Combining Model Predictive and Proportional-Integral Controllers. *Ind. Eng. Chem. Res.* **2019**, *58*, 4546–4559.
- (28) Lu, Z.; Sun, Y.; Liu, S.; Qian, Z.; Chen, H.; Wu, S.; Zheng, J. Fuzzy-Logic-Based Modeling and Control for HiGee-AOP Nitric

Oxide Attenuation with a Complex Gas-Liquid Mass-Transfer-Reaction Process. *Ind. Eng. Chem. Res.* **2022**, *61*, 3428–3438.

(29) Xu, G. X. *Rare Earths*; Metallurgical Industry Press: Beijing, 2012.

(30) Jia, W. J. *Modeling and Intelligent Optimal Control for Rare Earth Extraction Process*; Shenyang, Northeastern University, 2007.

(31) Sun, B.; Zhang, B.; Yang, C. H.; Gui, W. H. Discussion on Modeling and Optimal Control of Nonferrous Metallurgical Purification Process. *Acta Autom. Sin.* **2017**, *43* (6), 880–892.

(32) Gui, W. H.; Yang, C. H.; Chen, X. F.; Wang, Y. L. Modeling and Optimization Problems and Challenges Arising in Nonferrous Metallurgical Processes. *Acta Autom. Sin.* **2013**, *39* (3), 197–207.